DEVELOPMENTAL BIOLOGY

An essential role for $G\alpha_{i2}$ in Smoothened-stimulated epithelial cell proliferation in the mammary gland

Hugo Villanueva,[1,2] Adriana P. Visbal,[1,2]* Nadine F. Obeid,[2] Andrew Q. Ta,[2] Adeel A. Faruki,[2] Meng-Fen Wu,[2] Susan G. Hilsenbeck,[2,3] Chad A. Shaw,[4] Peng Yu,[5] Nicholas W. Plummer,[6] Lutz Birnbaumer,[6†] Michael T. Lewis[1,2,7‡]

Hedgehog (Hh) signaling is critical for organogenesis, tissue homeostasis, and stem cell maintenance. The gene encoding Smoothened (SMO), the primary effector of Hh signaling, is expressed aberrantly in human breast cancer, as well as in other cancers. In mice that express a constitutively active form of SMO that does not require Hh stimulation in mammary glands, the cells near the transgenic cells proliferate and participate in hyperplasia formation. Although SMO is a seven-transmembrane receptor like G protein–coupled receptors (GPCRs), SMO-mediated activation of the Gli family of transcription factors is not known to involve G proteins. However, data from *Drosophila* and mammalian cell lines indicate that SMO functions as a GPCR that couples to heterotrimeric G proteins of the pertussis toxin (PTX)–sensitive $G\alpha_i$ class. Using genetically modified mice, we demonstrated that SMO signaling through G proteins occurred in the mammary gland in vivo. SMO-induced stimulation of proliferation was PTX-sensitive and required $G\alpha_{i2}$, but not $G\alpha_{i1}$, $G\alpha_{i3}$, or activation of Gli1 or Gli2. Our findings show that activated SMO functions as a GPCR to stimulate proliferation in vivo, a finding that may have clinical importance because most SMO-targeted agents have been selected based largely on their ability to block Gli-mediated transcription.

INTRODUCTION

The Hedgehog (Hh) signaling network controls key aspects of metazoan development including cell fate, tissue patterning, and proliferation (*1*, *2*). Hh signaling perturbations cause developmental defects such as cyclopia and polydactyly, and increased signaling is implicated in cancers including those of the skin, brain, and breast (*3*–*13*).

In the absence of an Hh ligand, Smoothened (SMO) is functionally inhibited by the Hh receptor Patched-1 (Ptch1) or Patched-2 (Ptch2). SMO inhibition leads to the repression of target gene expression by production of transcriptional repressor forms of the Gli transcription factors. In the presence of an Hh ligand, Hh will bind to Ptch1 or Ptch2 with the aid of a co-receptor system composed of Commodo, Brother of Commodo, and Gas1 to promote release of SMO inhibition (*14*, *15*). SMO activation allows production of the transcriptional activator forms of the Gli transcription factors, which promote target gene expression (*16*).

SMO is homologous with seven-pass transmembrane G protein (heterotrimeric guanine nucleotide–binding protein)–coupled receptors (GPCRs), but data supporting G protein coupling in vivo have been lacking. Genetic analyses in *Drosophila* have demonstrated that $G\alpha_i$-protein coupling is essential for canonical Smo-mediated Hh signal transduction (*17*). Smo GPCR function in *Drosophila* demonstrates that signaling varies slightly from its vertebrate counterpart. Ogden and colleagues have shown that in *Drosophila*, the presence of Hh promotes recruitment of $G\alpha_i$ to a complex with Smo, a process that is facilitated by the kinesin-related protein Cos2. Once in a complex with Smo, $G\alpha_i$ activation leads to a reduction in intracellular adenosine 3′,5′-monophosphate (cAMP) concentration and presumably reduces protein kinase A activation (*17*). In cultured mammalian cells, SMO can couple with several Gα subunits including the pertussis toxin (PTX)–sensitive $G\alpha_{i1}$, $G\alpha_{i2}$, $G\alpha_{i3}$, and $G\alpha_o$ (*17*–*21*). PTX functions by adenosine diphosphate–ribosylating $G\alpha_{i/o}$ proteins to prevent GPCR coupling. It blocks pigment aggregation in *Xenopus laevis* melanophores, an SMO-mediated process, suggesting an SMO-$G\alpha_i$ interaction (*22*). Whether SMO can function as a GPCR in vivo in mammals has not been demonstrated.

We have previously shown that Cre-recombinase dependent expression of constitutively active SMO (hereinafter $SmoM2^c$) in mammary epithelial cells promotes proliferation in a paracrine or juxtacrine manner and that $SmoM2^c$-overexpressing cells show evidence of Hh pathway activation (*13*, *23*). Here, we provide evidence that $SmoM2^c$ can function as a GPCR that requires the heterotrimeric G protein $G\alpha_{i2}$ and that $SmoM2^c$-induced proliferation appears to occur independently of Gli1 or Gli2 transcription factor function.

RESULTS

In vivo treatment with PTX suggests involvement of one or more PTX-sensitive G proteins

To determine whether SMO might promote mammary epithelial cell proliferation in vivo through one or more PTX-sensitive $G\alpha_i$ proteins, we induced the expression of $SmoM2^c$, as well as recombination of the Cre-dependent

[1]Department of Molecular and Cellular Biology, Baylor College of Medicine, Houston, TX 77030, USA. [2]Lester and Sue Smith Breast Center, Baylor College of Medicine, Houston, TX 77030, USA. [3]Department of Medicine, Baylor College of Medicine, Houston, TX 77030, USA. [4]Department of Molecular and Human Genetics, Baylor College of Medicine, Houston, TX 77030, USA. [5]Department of Electrical and Computer Engineering, TEES-AgriLife Center for Bioinformatics and Genomic Systems Engineering, Texas A&M University, College Station, TX 77843, USA. [6]Neurobiology Laboratory, National Institute of Environmental Health Sciences, National Institutes of Health, Research Triangle Park, NC 27709, USA. [7]Department of Radiology, Baylor College of Medicine, Houston, TX 77030, USA.
*Present address: Department of Natural Sciences, University of Houston-Downtown, Houston, TX 77002, USA.
†Present address: Instituto de Investigaciones Biotecnológicas–Instituto Tecnológico de Chascomús (IIB-INTECH), Universidad Nacional de San Martín, San Martín CP1650, Argentina.
‡Corresponding author. E-mail: mtlewis@bcm.edu

dual-fluorescence reporter *mT-mG*, through intraductal injection of adenovirus-expressing Cre recombinase (ad-Cre) (*23*, *24*). Ad-Cre–mediated recombination of *SmoM2*^{c} in a subset of ductal epithelial cells was indicated by enhanced green fluorescent protein (EGFP) expression from the recombined *mT-mG* allele, whereas *SmoM2*^{c}-negative cells lacking recombination remained tdTomato-positive (see Materials and Methods for details). Adenovirus-lacZ (ad-lacZ) was injected in the contralateral mammary gland as a negative control. We subsequently treated mice with PTX or phosphate-buffered saline (PBS) vehicle control and evaluated proliferation by bromodeoxyuridine (BrdU) incorporation.

Control mammary glands infected with ad-lacZ and treated with PBS showed proliferation rates consistent with those of mammary glands from normal adult virgin mice (Fig. 1A). In contralateral ad-Cre–infected, PBS-treated mammary glands, *SmoM2*^{c} expression led to increased proliferation in *SmoM2*^{c}-negative cells (Fig. 1B), consistent with previous results (*23*). In contrast, PTX impaired the proliferative response to *SmoM2*^{c} such that there was no difference between ad-lacZ– and ad-Cre–treated animals (Fig. 1, C and D, PTX group). Quantification of BrdU incorporation for each group is displayed in Fig. 1E.

PTX attenuates SMO-induced proliferation ex vivo

Because PTX treatment in vivo may cause systemic changes that could confound the analysis, we sought to determine whether PTX could act directly on the mammary gland using cultured explants. Mammary gland explants derived from 5-week-old *mT-mG/SmoM2*^{c}*;MMTV-Cre* and *mT-mG/SmoM2*^{c}*;+* (Cre-negative) littermates were maintained in organ culture ex vivo and treated with either PBS or PTX and pulsed with BrdU. In this system, *SmoM2*^{c} expression was achieved through a genetic cross to an MMTV-Cre transgenic mouse that expresses Cre recombinase in a mammary-selective manner under the control of the mouse mammary tumor virus (MMTV) long terminal repeat promoter, rather than by ad-Cre injection. The control *mT-mG/SmoM2*^{c}*;+* explants treated with PBS showed proliferation rates expected for ducts in a 5-week-old gland (Fig. 1F). Explants with MMTV-Cre–mediated *SmoM2*^{c} recombination (as indicated by EGFP fluorescence) displayed increased proliferation (Fig. 1G). Consistent with the results of our in vivo experiment, PTX abolished *SmoM2*^{c}-induced proliferation with no difference between *mT-mG/SmoM2*^{c}*;+* and *mT-mG/SmoM2*^{c}*;MMTV-Cre* explants (Fig. 1, H and I), demonstrating that the effects of PTX were not due to a systemic influence on the mammary gland. The quantification of BrdU incorporation for each group is displayed in Fig. 1J.

PTX does not affect ovarian hormone– or pregnancy-induced mammary epithelial cell proliferation

To evaluate whether PTX could block steroid hormone–induced proliferation, we induced mammary epithelial cell proliferation in wild-type female mice with combined estrogen (E_2) and progesterone (P_4) treatment (compared to sesame oil vehicle) and concurrently administered either PTX or PBS vehicle control. Treatment with E_2 and P_4 in conjunction with PBS led to an increase in cell division compared with sesame oil–treated mice (Fig. 2A compared to Fig. 2B). This increase in proliferation was not blocked by PTX (Fig. 2, C to E, and table S1).

To test PTX specificity for *SmoM2*^{c}-induced proliferation further, we treated pregnant mice with either PBS vehicle control or PTX. Consistent with the steroid hormone treatment, pregnancy-induced proliferation was unaffected by PBS (Fig. 2F) and was not blocked by PTX (Fig. 2G). The quantification of BrdU incorporation is displayed in Fig. 2H and table S1.

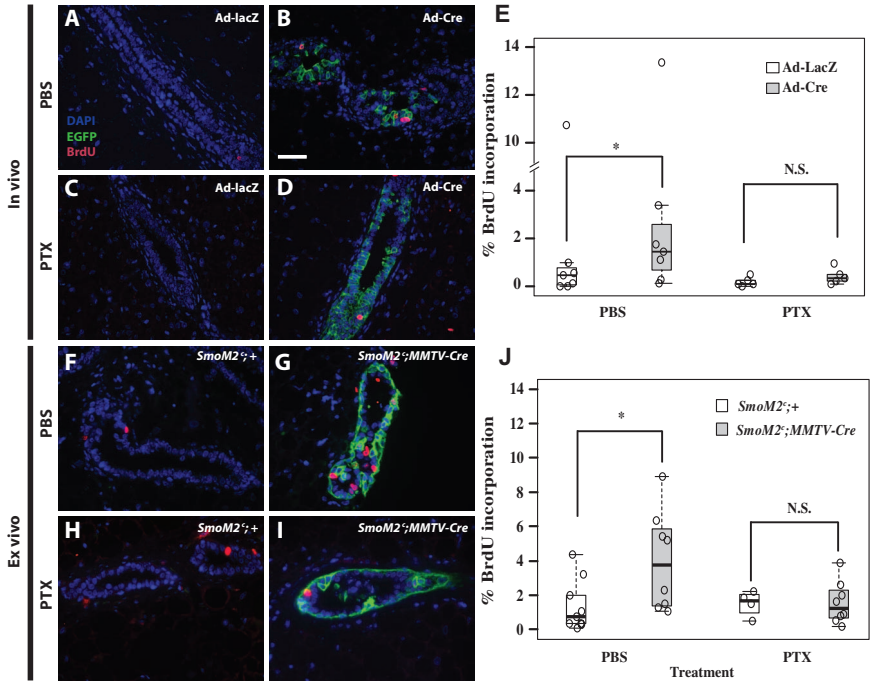

Fig. 1. PTX blocks SmoM2^{c}-induced proliferation in vivo and ex vivo. (A to D) In vivo: BrdU and EGFP co-immunofluorescence in PBS-treated *mT-mG/SmoM2*^{c} mice intraductally injected in contralateral mammary glands with either ad-lacZ (A) or ad-Cre (B) (n = 7 mice), as well as PTX treatment of mice intraductally injected with ad-lacZ (C) or ad-Cre (D) (n = 5 mice). (E) Percent BrdU incorporation in ad-lacZ– or ad-Cre–injected *SmoM2*^{c} mice treated with PBS vehicle or PTX. N.S., not statistically significant. (F to I) Ex vivo: BrdU and EGFP co-immunofluorescence in PBS-treated organ cultures *SmoM2*^{c}*;+* (n = 9 explants) (F) or *SmoM2*^{c}*;MMTV-Cre* (n = 8 explants) (G) and in organ cultures treated with PTX: *SmoM2*^{c}*;+* (n = 4 explants) (H) and *SmoM2*^{c}*;MMTV-Cre* (n = 8 explants) (I). (J) Percent BrdU incorporation in *SmoM2*^{c}*;+* and *SmoM2*^{c}*;MMTV-Cre* organ cultures treated with PBS vehicle and PTX. *P < 0.05 was determined by Wilcoxon signed rank (in vivo) and rank-sum (ex vivo) tests. Box plots represent median, interquartile range, and minimum and maximum values. Scale bar, 50 μm.

Genes encoding PTX-sensitive Gα$_{i}$ subunits are expressed in mammary epithelial cells, and the expression of the gene encoding Gα$_{i1}$ is specifically increased by SmoM2^{c}

The ability of PTX to selectively block *SmoM2*^{c}-induced proliferation suggested involvement of PTX-sensitive Gα subunit(s) of heterotrimeric G proteins. To determine whether expression of genes encoding Gα subunits was altered as a function of *SmoM2*^{c} expression, we interrogated RNA sequencing (RNA-seq) data comparing mammary epithelial cell populations derived from *mT-mG/SmoM2*^{c}*;MMTV-Cre* and *mT-mG/SmoM2*^{c}*;+* mammary glands. Recombined

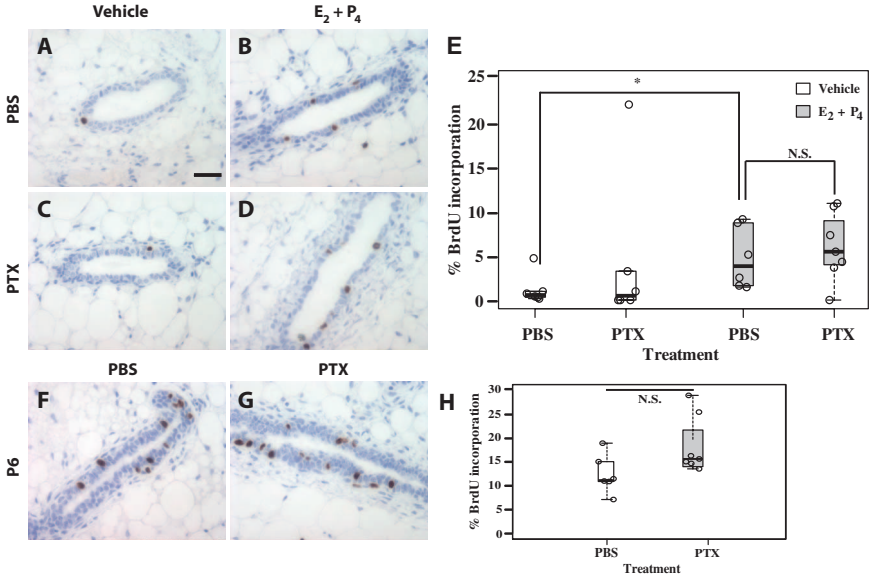

Fig. 2. PTX does not affect proliferation induced by steroid hormones ($E_2 + P_4$) or pregnancy. (A to D) BrdU staining of mouse mammary glands from wild-type (WT) virgin mice treated with sesame oil (vehicle for $E_2 + P_4$) and PBS (vehicle for PTX) ($n = 6$ mice) (A), $E_2 + P_4$ and PBS ($n = 6$ mice) (B), sesame oil and PTX ($n = 6$ mice) (C), or $E_2 + P_4$ and PTX ($n = 7$ mice) (D). (E) Percent BrdU incorporation in sesame oil– or $E_2 + P_4$–treated mice in conjunction with PBS or PTX. (F and G) BrdU staining of mouse mammary glands from 6-day pregnant adult WT mice treated with PBS ($n = 6$ mice) (F) and PTX ($n = 7$ mice) (G). (H) Percent BrdU incorporation in 6-day pregnant mice treated with PBS/PTX. *$P < 0.05$ (determined by Wilcoxon rank-sum test). Box plots represent median, interquartile range, and minimum and maximum values. P6, pregnancy day 6. Scale bar, 40 μm.

SmoM2^c-expressing (EGFP) and unrecombined (tdTomato) mammary epithelial cells derived from *mT-mG/SmoM2^c;MMTV-Cre* mice, and wild-type (tdTomato) mammary epithelial cells isolated from *mT-mG/SmoM2^c;+* littermates were enriched by fluorescence-activated cell sorting (FACS). mRNA derived from each population was used for RNA-seq analysis. tdTomato mammary epithelial cells from *mT-mG/SmoM2^c*;+ mice were used as the "wild-type" control to identify genes that were differentially regulated in response to *SmoM2^c* expression.

Overall, mRNAs encoding 15 Gα subunits were detectably expressed, including all known PTX-sensitive Gα subunits. Of these, the mRNA encoding the PTX-sensitive $G\alpha_{i1}$ subunit was the only transcript that showed increased expression as a consequence of *SmoM2^c* expression (Fig. 3A). The expression of genes encoding PTX-sensitive $G\alpha_i$ ($G\alpha_{i1}$, $G\alpha_{i2}$, and $G\alpha_{i3}$) subunits was validated by quantitative reverse transcription polymerase chain reaction (qRT-PCR) using two independent primer sets for each gene (Fig. 3B). These expression data suggested that $G\alpha_{i1}$ was the most likely candidate for mediating the effects of *SmoM2^c* but did not rule out $G\alpha_{i2}$ and $G\alpha_{i3}$ because the genes encoding these Gα subunits were the most highly expressed of those encoding PTX-sensitive Gα subunits.

SmoM2^c-induced mammary gland proliferation requires PTX-sensitive $G\alpha_{i2}$

To test the hypothesis that at least one of these $G\alpha_i$ subunits mediates *SmoM2^c*-induced proliferation, we crossed *mT-mG* or *SmoM2^c* homozygous mice with mice homozygous for null alleles of $G\alpha_{i1}$ and $G\alpha_{i3}$, as well as a conditional allele of $G\alpha_{i2}$ ($G\alpha_{i1}^{-/-}$; $G\alpha_{i2}^{f/f}$; $G\alpha_{i3}^{-/-}$). Offspring were intercrossed to generate *mT-mG*–tagged animals heterozygous for *SmoM2^c* and homozygous for a single $G\alpha_i$ mutation (fig. S1). *SmoM2^c* and *EGFP* expression, as well as deletion of the $G\alpha_{i2}$ conditional allele, were achieved by intraductal injection of ad-Cre. An ad-lacZ injection was used as a negative control in the contralateral mammary gland.

In ad-lacZ–injected negative control mammary glands carrying wild-type alleles of $G\alpha_{i1}$, $G\alpha_{i2}$, and $G\alpha_{i3}$, baseline proliferation was low, consistent with that of an adult wild-type mouse (Fig. 4A). Conversely, in positive control glands, *SmoM2^c* expression in the presence of all three wild-type $G\alpha_i$ alleles increased mammary gland proliferation (Fig. 4B), as expected. In the ad-lacZ control group, $G\alpha_{i1}$ disruption did not alter baseline proliferation (Fig. 4C), although heterozygous deletion of one $G\alpha_{i1}$ allele led to an unexpected increase in proliferation (fig. S2). Contrary to our hypothesis, homozygous $G\alpha_{i1}$ disruption failed to attenuate *SmoM2^c*-induced proliferation (Fig. 4, D and E).

In homozygous $G\alpha_{i2}^{f/f}$ animals, ad-Cre injection led to disruption of $G\alpha_{i2}$ ($G\alpha_{i2}^{d/d}$) in EGFP/SmoM2^c-positive cells and, in contrast with $G\alpha_{i1}$ disruption, completely abolished *SmoM2^c*-induced paracrine proliferation (Fig. 4, F to H). The conditional ablation of $G\alpha_{i2}$ in the absence of a *SmoM2^c* allele did not affect baseline proliferation (fig. S2 and table S2). Thus, $G\alpha_{i2}$ function is required in *SmoM2^c*-expressing cells themselves to stimulate proliferation in neighboring, unrecombined *SmoM2^c*-negative cells. In contrast, $G\alpha_{i3}$ disruption did not affect *SmoM2^c*-induced proliferation (Fig. 4, I to K).

SmoM2^c-induced mammary gland proliferation does not appear to require Gli1 or Gli2 transcription factor function

Previous data indicate that Gli transcription factors are increased in SmoM2^c-expressing tissues (*23*). To test whether Gli-mediated signaling contributed to SmoM2^c-driven proliferation, we treated *mT-mG/SmoM2^c* mice intraductally infected with ad-Cre and ad-lacZ with the Gli1 and Gli2 antagonist GANT61 (*25*). As a positive control for GANT61 activity, we tested its specificity in vivo using the uterine artificially induced decidual response, which requires Hh signaling (*26*). The difference in the decidual response was quantified by measuring the weight ratio of the decidual horn (left horn) to the control horn (right horn).

Vehicle-treated mice experienced a robust response on the horn that underwent decidual trauma (left horn) compared to the unstimulated horn (right horn) (Fig. 5A). GANT61 completely blocked the decidual response such that there was no difference between the decidual and control horns (Fig. 5, A and B). To determine whether Gli transcription factor target genes were affected by GANT61 treatment, we performed qRT-PCR analysis and found that GANT61 reduced the expression of Hh pathway autoregulated genes *Ptch1*, *Gli1*, *Gli2*, and *Hhip* (Fig. 5C), thereby confirming the specificity of GANT61.

We next analyzed mammary gland proliferation in *SmoM2^c* mice treated with vehicle and GANT61. In mice that received vehicle, proliferation was increased in ad-lacZ compared to ad-Cre groups, as expected (Fig. 5, D and E). Treatment with GANT61 did not block increased proliferation in the

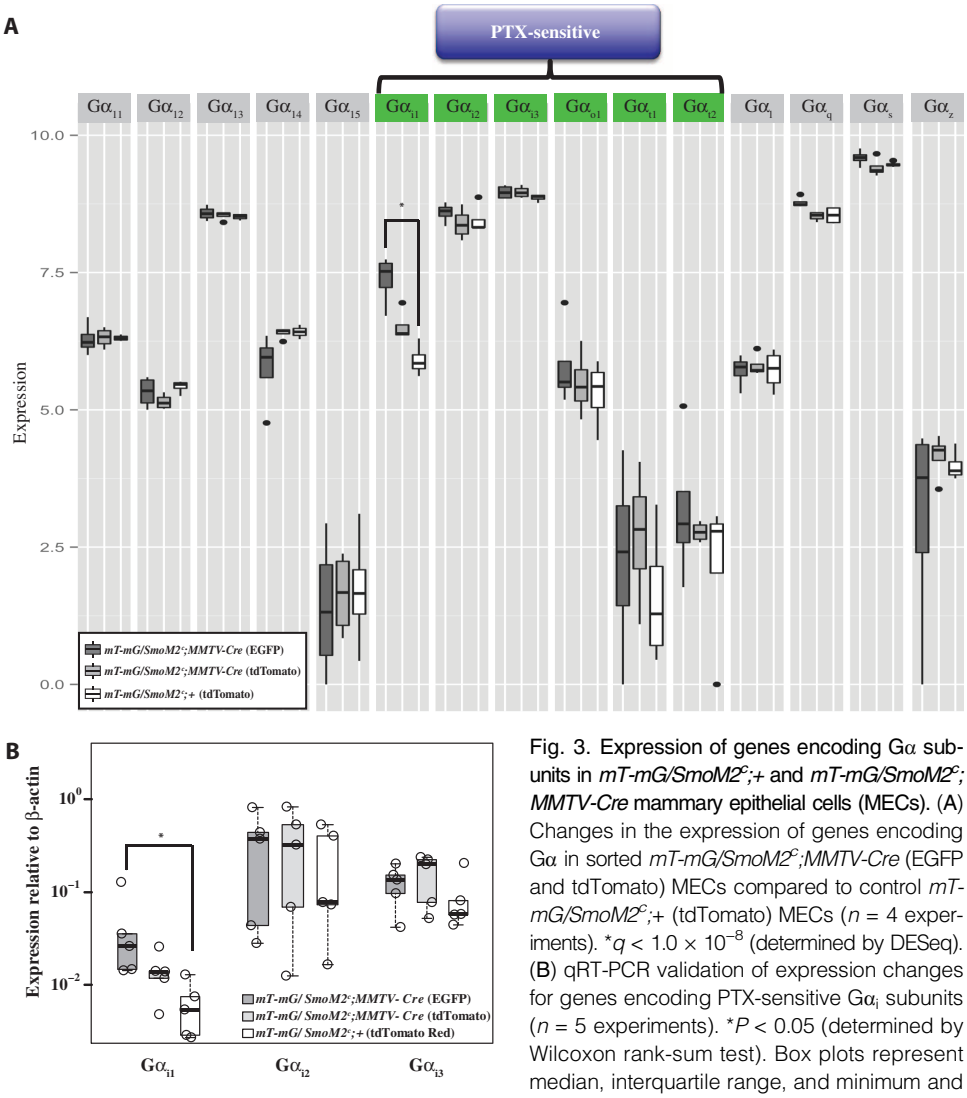

Fig. 3. Expression of genes encoding Gα subunits in *mT-mG/SmoM2^c;+* and *mT-mG/SmoM2^c;MMTV-Cre* mammary epithelial cells (MECs). (A) Changes in the expression of genes encoding Gα in sorted *mT-mG/SmoM2^c;MMTV-Cre* (EGFP and tdTomato) MECs compared to control *mT-mG/SmoM2^c;+* (tdTomato) MECs (n = 4 experiments). *$q < 1.0 \times 10^{-8}$ (determined by DESeq). (B) qRT-PCR validation of expression changes for genes encoding PTX-sensitive $G\alpha_i$ subunits (n = 5 experiments). *$P < 0.05$ (determined by Wilcoxon rank-sum test). Box plots represent median, interquartile range, and minimum and maximum values; filled ovals represent outliers.

ad-lacZ group compared with the ad-Cre group (Fig. 5, F and G), ruling this pathway out as a potential mediator of paracrine proliferation. BrdU incorporation was quantified, and results are displayed in Fig. 5H and fig. S3.

SmoM2^c expression increases the expression of genes involved in cytoskeletal regulation, G protein signaling, Wnt signaling, planar cell polarity, and axon guidance signaling

To elucidate the potential pathways driving the *SmoM2^c*-induced paracrine stimulation of proliferation, we used literature investigation and Ingenuity Pathway Analysis to identify multiple genes and pathways affected by *SmoM2^c* expression from the RNA-seq data set in *mT-mG/SmoM2^c;MMTV-Cre* (recombined EGFP) and *mT-mG/SmoM2^c;MMTV-Cre* (unrecombined tdTomato) mammary epithelial cells relative to *mT-mG/SmoM2^c;+* (wild-type tdTomato) mammary epithelial cells (table S5). This approach allowed for an overview of how *SmoM2^c*-expressing (recombined EGFP) cells could be communicating with their neighboring *SmoM2^c*-negative (unrecombined tdTomato) cells to promote their proliferation.

Pathway analysis of genes that showed increased expression only in recombined EGFP cells indicated enhanced expression of some genes involved in cytoskeletal regulation and in G protein signaling (fig. S4). Furthermore, we found that genes involved in Hh and Notch signaling pathways showed increased expression only in recombined EGFP cells, consistent with our previously published results (*23*). Additionally, genes in the Wnt signaling/planar cell polarity pathways, which may participate in the *SmoM2^c*-promoted alveolar budding phenotypes observed here and/or in previous findings (*23*), also showed increased expression. *SmoM2^c* expression caused the decreased expression of hormone receptor genes (*Esr1*, *Pgr*, and *Prlr*) and increased the expression of genes associated with mammary epithelial cell differentiation (*Csn1s2a*, *Csn2*, and *Btn2a2*).

To gain insight into the response of unrecombined tdTomato mammary epithelial cells to recombined EGFP cells, we analyzed the genes and pathways that showed increased expression only in the tdTomato cells (yellow-colored genes) as well as those that showed decreased expression in recombined EGFP cells and increased expression in unrecombined tdTomato cells (magenta-colored genes). This gene level and pathway analysis revealed that genes encoding collagens showed increased expression in unrecombined tdTomato cells in addition to decreased expression in recombined EGFP cells and increased expression in unrecombined tdTomato cells (fig. S4).

Recombined EGFP cells had a large number of genes with a marked increase in expression of those encoding factors involved in axon guidance, which included multiple signaling pathways such as Slit-Robo signaling (*Robo1* and *Srgap1*), ephrin-ephrin receptor signaling (*Epha7*, *Ephb1*, and *Ephb7*), semaphorin-plexin signaling (*Plxna1*), and neurotrophic signaling (*Ntrk3*, *Ntf4*, and *Bdnf*) (fig. S4). We found that the expression of the genes encoding the receptors for these different axon guidance pathways showed increased expression in the responding unrecombined tdTomato cells and, although not differentially regulated, genes encoding downstream effectors such as Ras and RhoA signaling axes were expressed in unrecombined tdTomato cells. Analysis of genes encoding receptors that are not involved in axon guidance and that showed increased expression in the unrecombined tdTomato cells revealed many membrane-bound receptors that could be signaling within this population of cells to promote cell proliferation. These receptors include the $G\alpha_i$-coupled GPCR-encoding genes *Lpar1* and *Slpr3*, the $G\alpha_s$-coupled receptor-encoding gene *Calcrl*, and the GPCR-encoding gene *Ptgfr* (fig. S4).

DISCUSSION

We report here that SMO-induced paracrine stimulation of mammary epithelial cell proliferation was abolished by PTX, as well as by $G\alpha_{i2}$ disruption

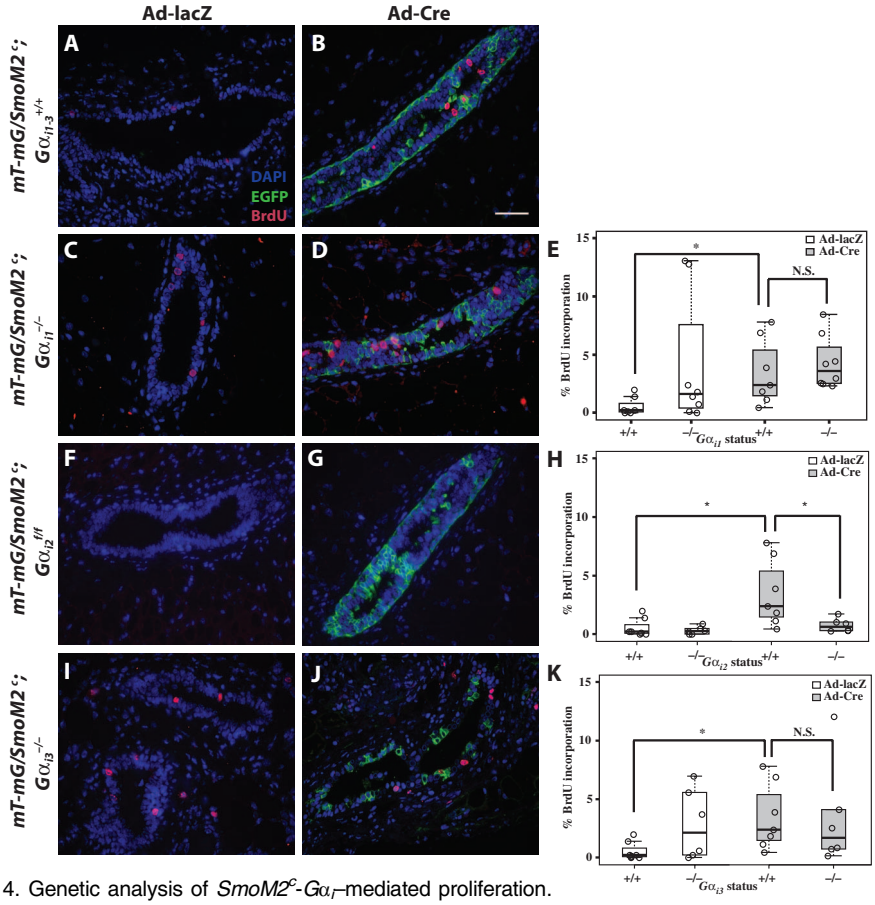

Fig. 4. Genetic analysis of *SmoM2*^{c}-$G\alpha_i$–mediated proliferation. (**A** to **D**) BrdU and GFP co-immunofluorescence in *mT-mG/SmoM2*^{c};$G\alpha_i^{+/+}$ mice intraductally injected in contralateral mammary glands with either ad-lacZ (A) or ad-Cre (B) (n = 7 mice) and in *mT-mG/SmoM2*^{c} mice lacking $G\alpha_{i1}$ (*mT-mG/SmoM2*^{c};$G\alpha_{i1}^{-/-}$) and intraductally injected in contralateral mammary glands with either ad-lacZ (C) or ad-Cre (D) (n = 8 mice). (**E**) Percent BrdU incorporation *in mT-mG/SmoM2*^{c};$G\alpha_i^{+/+}$ and *mT-mG/SmoM2*^{c};$G\alpha_{i1}^{-/-}$ groups. (**F** and **G**) BrdU and GFP co-immunofluorescence in *mT-mG/SmoM2*^{c} mice conditionally lacking $G\alpha_{i2}$ (*mT-mG/SmoM2*^{c};$G\alpha_{i2}^{f/f}$) and intraductally injected in contralateral mammary glands with either ad-lacZ (F) or ad-Cre (*mT-mG/SmoM2*^{c};$G\alpha_{i2}^{d/d}$) (G) (n = 6 mice) (f/f denotes the unrecombined floxed allele, and d/d denotes the recombined allele). (**H**) Percent BrdU incorporation in *mT-mG/SmoM2*^{c};$G\alpha_i^{+/+}$ and *mT-mG/SmoM2*^{c};$G\alpha_{i2}^{f/f}$ and *mT-mG/SmoM2*^{c};$G\alpha_{i2}^{d/d}$ groups. (**I** and **J**) BrdU and GFP co-immunofluorescence in *mT-mG/SmoM2*^{c} mice lacking $G\alpha_{i3}$ (*mT-mG/SmoM2*^{c};$G\alpha_{i3}^{-/-}$) in ad-lacZ–infected (I) and ad-Cre–infected (J) mammary ducts (n = 6 mice). (**K**) Percent BrdU incorporation in *mT-mG/SmoM2*^{c};$G\alpha_i^{+/+}$ and *mT-mG/SmoM2*^{c};$G\alpha_{i3}^{-/-}$ groups. *P < 0.05 [determined by Wilcoxon signed rank test (for paired ad-lacZ compared to ad-Cre) and Wilcoxon rank-sum test (for unpaired ad-Cre–treated $G\alpha_i$ WT compared to $G\alpha_i$ deletion mutants)]. Box plots represent median, interquartile range, and minimum and maximum values. Scale bar, 50 μm.

in *SmoM2*^{c}-expressing cells themselves, revealing a cell-autonomous requirement for $G\alpha_{i2}$. These data indicated that $G\alpha_{i2}$ was necessary to mediate SMO-induced proliferation and that no other $G\alpha_i$ subunit compensated for its loss. Further, our GANT61 results suggested that mammary gland proliferation as a consequence of *SmoM2*^{c} expression did not depend on Gli1 or Gli2 transcription factor function.

Our current findings agree with previous publications that suggest that SmoM2 couples with and activates $G\alpha_{i2}$, and with studies that demonstrate that $G\alpha_{i2}$ is one of the $G\alpha_i$ subunits required for Shh-induced proliferation in cerebellar granular neuronal precursor cells (*19*, *21*). Additionally, our results fit with data demonstrating that SmoM2-mediated Hh signaling, which is blocked by PTX, is rescued by expression of a mutant $G\alpha_{i2}$ that fails to hydrolyze guanosine triphosphate (*19*), supporting the notion that this is indeed a $G\alpha_{i2}$-mediated process. However, unlike previous findings in cerebellar, granular neuronal precursor cells suggesting interchangeability of $G\alpha_{i2}$ and $G\alpha_{i3}$ function, our work demonstrated that the function of these subunits was not interchangeable when promoting *SmoM2*^{c}-induced proliferation in the mammary gland. This difference could be explained if wild-type SMO can couple with multiple $G\alpha_i$ subunits, whereas constitutively active SmoM2 prefers to couple exclusively to $G\alpha_{i2}$. Although Hh signaling through SMO G protein–mediated function can occur in conjunction with Gli transcription factor activity (*17*, *19*), our results suggested that Gli1- or Gli2-mediated transcription was dispensable for paracrine-stimulated proliferation by *SmoM2*^{c}, a finding consistent with Hh-mediated angiogenic responses in endothelial cells and migration in fibroblasts (*20*, *27*).

The dual-fluorescence mT-mG reporter allowed us to separate recombined EGFP cells expressing *SmoM2*^{c} from unrecombined tdTomato cells and to assess the unique transcriptional changes elicited by *SmoM2*^{c} expression that may account for the paracrine stimulation of proliferation observed in this model. Our gene expression data demonstrated that $G\alpha_{i1}$ showed increased expression as a consequence of *SmoM2*^{c} expression in mammary epithelial cells. We speculate that a potential explanation may be due to increased expression of genes encoding different adenylyl cyclases as a result of *SmoM2*^{c} overexpression. Increased $G\alpha_{i1}$ expression may be part of a negative feedback loop to modulate adenylyl cyclase activity. One interesting idea is that Gli transcription factors may be acting as transcriptional activators of $G\alpha_{i1}$; however, the $G\alpha_{i1}$ promoter lacks Gli binding sites and $G\alpha_{i1}$ has not been identified as a putative Gli transcriptional target in a previous analysis of Shh targets during neural patterning (*28*). These findings, coupled with the lack of useful antibodies to perform chromatin immunoprecipitation analysis, make $G\alpha_{i1}$ as a Gli target both unlikely and a difficult hypothesis to test.

Our Ingenuity Pathway Analysis identified candidate gene networks and signaling pathways (namely, Hh, Notch, and G protein signaling) modulated by *SmoM2*^{c} expression in EGFP cells. Of these, genes encoding axon guidance molecules, which are associated with tissue morphogenesis, cell adhesion, and proliferation in the mammary gland, were differentially regulated (mainly they showed increased expression) as a consequence of *SmoM2*^{c} overexpression in both recombined EGFP and unrecombined

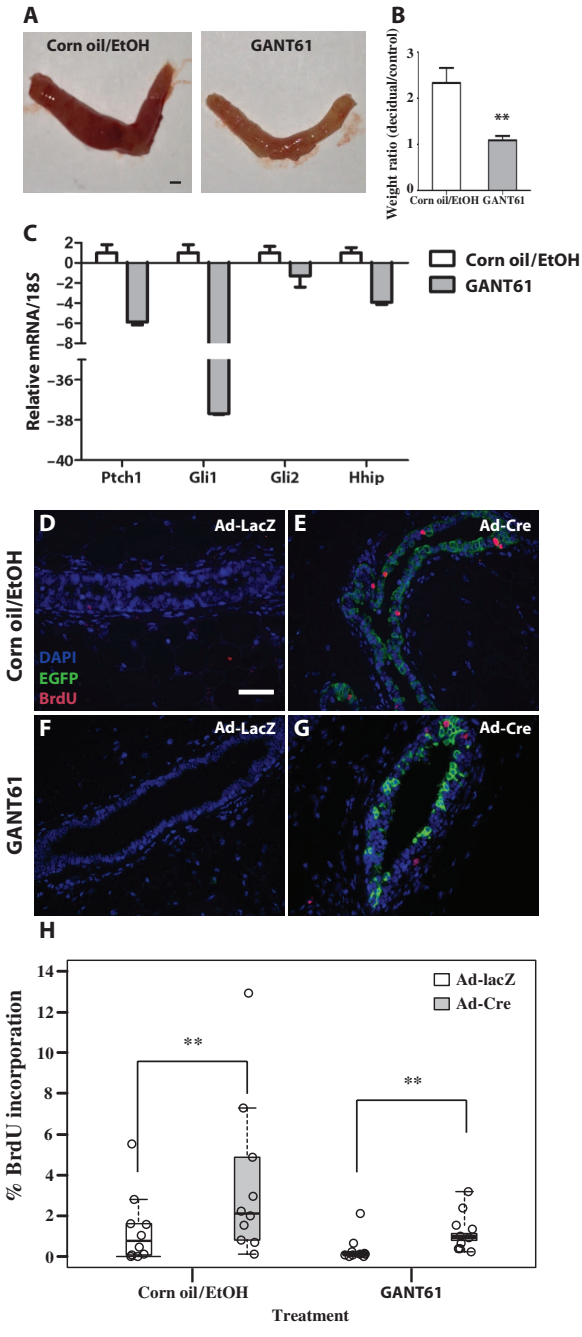

Fig. 5. GANT61 does not block SmoM2^{c}-induced proliferation in vivo. (**A**) Corn oil with ethanol (EtOH) vehicle and GANT61-treated WT mouse uterus 2 days after decidual trauma in the artificial decidual response. Decidual horn is on the left, and control horn is on the right. (**B**) Quantification of the decidual response (the weight ratios of the decidual to the control horn) 2 days after the decidual trauma in vehicle controls (n = 6 mice) compared to GANT61-treated mice (n = 5 mice). (**C**) qRT-PCR analysis of Hh autoregulated genes *Ptch1*, *Gli1*, *Gli2*, and *Hhip* 30 hours after E_2 and P_4 administration and corn oil/EtOH vehicle control or GANT61 treatment (n = 3 mice). (**D** to **G**) BrdU and EGFP co-immunofluorescence in corn oil/EtOH-treated *mT-mG*/*SmoM2*^{c} mice intraductally injected in contralateral mammary glands with either ad-lacZ (D) or ad-Cre (E) (n = 10 mice) and in GANT61-treated *mT-mG*/*SmoM2*^{c} mice intraductally injected with ad-lacZ (F) or ad-Cre (G) (n = 10 mice). (**H**) Percent BrdU incorporation in ad-lacZ– or ad-Cre–injected *SmoM2*^{c} mice treated with corn oil/EtOH vehicle or GANT61. $^{**}P < 0.01$ was determined by Wilcoxon rank-sum (B) and Wilcoxon signed rank (H) tests. Bars in (B) represent the mean, and error bars represent the SEM. Bars in (C) represent the mean, and error bars represent 95% confidence interval. Box plots in (H) represent median, interquartile range, and minimum and maximum values. Scale bars, 1 mm (A); 50 μm (D to G).

tdTomato cells. Previous data from our laboratory suggest that *SmoM2* overexpression in the mammary gland results in altered proliferation, disrupted histoarchitecture, and increased branching and budding of the ductal epithelium (*23*). These alterations in ductal growth and morphology could potentially be explained by disruption of axon guidance molecules, specifically those affecting Slit-Robo receptor biology, ephrin signaling, and semaphorin signaling as has been previously demonstrated by others (*29*–*31*). It would be interesting to compare the molecular basis of the branching and budding phenotypes observed in our *SmoM2* model to the molecular events transpiring during alveologenesis to determine whether similar mechanisms are used by mammary epithelial cells. Given the differential regulation of hormone receptor–encoding genes and genes normally expressed during alveolar differentiation in recombined EGFP cells (fig. S4), as well as the increased expression of stem cell–associated genes in unrecombined tdTomato cells, it would not be surprising that alveologenesis-like differentiation processes are being used because of altered SMO activity in the mammary gland.

In unrecombined tdTomato cells, increased expression of genes encoding several collagens was observed, which is consistent with previously observed changes in the extracellular matrix of *SmoM2*^{c}*;MMTV-Cre* mouse mammary glands, which include an increase in periductal collagen deposition (*23*). We hypothesize that this change could be due to the disruption in the luminal and myoepithelial layers that occurs with *SmoM2*^{c} overexpression (*23*). The gene level and pathway analysis has allowed us to identify potential ligand-receptor interactions between recombined EGFP and unrecombined tdTomato cells, specifically those of the Wnt pathway and axon guidance processes. The expression of *Bdnf*, *Ntf4*, and *Pdgfα*, which encode axon guidance signaling ligands, was increased in recombined EGFP cells, and the expression of *Ntrk2* and *Pdgfrα*/β, which encode the receptors for these ligands, was increased in unrecombined tdTomato cells. These receptors signal through Ras/Raf/MAPK (mitogen-activated protein kinase) pathways, which are mitogenic, and thus, these results could explain the paracrine-mediated increase in proliferation. Such pathways could be functionally tested in the future with small-molecule inhibitors such as cabozantinib, sunitinib, or telatinib.

One caveat in our analysis includes the strategy that was used to isolate the unrecombined tdTomato mammary epithelial cells. We used the mT-mG reporter to isolate the unrecombined cells from the *mT-mG*/*SmoM2*^{c}*;MMTV-Cre* population, which includes not only all proliferating tdTomato cells but also those nonproliferating cells, which make up the majority of the cell population. This strategy might dilute transcripts that were expressed exclusively in the proliferating cells and prevent us from identifying the key signaling pathways activated in these dividing cells.

Our study provides insight that could be translated toward the development of better therapeutic anticancer agents that target wild-type and mutant SMO and perhaps partially addresses the issue of resistance seen with several of these SMO antagonists. If human SMO activation in cancers uses a G protein pathway simultaneously with, or independently of, GLI signaling to drive tumor behavior, then SMO antagonists screened solely on the basis of their ability to block GLI-mediated transcriptional

activation may be suboptimal. It would be useful to assess Hh signaling in clinical specimens from patients who suffer from cancers displaying aberrant Hh signaling such as basal cell carcinomas or medulloblastomas that do not respond to current SMO antagonists to determine whether the G protein pathway is in fact activated.

Of relevance in breast cancer, the data presented in this study may be particularly relevant to the 70% of noninvasive ductal carcinoma in situ and 30% of invasive breast cancers that display ectopic expression of SMO (*13*). SMO expression in these breast cancers may contribute to the maintenance of subclonal heterogeneity required to promote non–cell-autonomous proliferation in tumors, a hypothesis confirmed in models of breast cancer (*32*). Collectively, our data support a model of paracrine-mediated interactions in the context of normal tissue development as well as tumor maintenance and suggest that Hh-driven proliferative phenotypes in other organs and structures should be reevaluated with respect to a potential role for $G\alpha_i$.

MATERIALS AND METHODS

Animal models

Mouse lines Gt(ROSA)26Sor$^{tm1(Smo/YFP)Amc}$/J carrying a Cre-dependent knock-in allele of *SmoM2* at the ROSA26 locus (herein designated SmoM2^c), and Gt(ROSA)26Sor$^{tm4(ACTB-tdTomato,\ -EGFP)Luo}$/J carrying the mT-mG dual-fluorescence Cre recombinase reporter targeted to the ROSA26 locus (herein designated mT-mG) were obtained from The Jackson Laboratory (stock #005130 and #007576, respectively). The lines were maintained as homozygotes in the original 129X1/SvJ, C57BL/6, and Swiss Webster mixed strain (*SmoM2^c* mice) or in a mixed genetic background (mT-mG mice). The MMTV-Cre (*33*) line (expressing Cre recombination under the control of the mammary-selective MMTV promoter) was a gift from T. Lane (University of California, Los Angeles, Los Angeles, CA) and was maintained as a hemizygous transgene in a mixed genetic background. $G\alpha_i$ mouse lines (*34*) were transferred from the Comparative Medicine Branch, National Institute of Environmental Health Sciences (Research Triangle Park, NC). Genotyping for all alleles was carried out by allele-specific PCR using primers listed in table S3.

MMTV-Cre mice were crossed with the *mT-mG* reporter line, and the offspring were intercrossed to generate males homozygous for *mT-mG* and hemizygous for MMTV-Cre, for use in subsequent crosses. *mT-mG*–tagged *SmoM2^c* (that is, *mT-mG/SmoM2^c*) mice were generated by crossing homozygous *SmoM2^c* females to homozygous *mT-mG* males. Experimental mice expressing *MMTV-Cre* and wild-type littermates (*mT-mG/SmoM2^c;MMTV-Cre* and *mT-mG/SmoM2^c*;+) were generated by crossing *SmoM2^c* homozygous females to males homozygous for *mT-mG* and hemizygous for the *MMTV-Cre* transgene. *mT-mG/SmoM2^c* mice with either $G\alpha_{i1}$, $G\alpha_{i2}$, or $G\alpha_{i3}$ disruption were initially generated by crossing either *mT-mG/mT-mG* or *SmoM2^c/SmoM2^c* homozygotes to 129SvEv- $G\alpha_{i1}^{-/-}$; $G\alpha_{i2}^{f/f}$; $G\alpha_{i3}^{-/-}$ mice. Offspring were then intercrossed, and subsequent offspring of desired genotypes were bred to each other to generate mice with the *mT-mG* and *SmoM2^c* alleles as well as the single $G\alpha_i$ knockouts and wild-type littermate controls (fig. S1). Single knock-out mice were then infected intraductally with ad-Cre recombinase and contralaterally with a negative control adenovirus expressing lacZ. Knock-in mice with both the *mT-mG* and *SmoM2^c* alleles allowed recombined cells expressing the *SmoM2^c* transgene to be tagged with EGFP, whereas surrounding cells that did not undergo recombination remained tdTomato-positive. All animals were maintained in accordance with the National Institutes of Health *Guide for the Care and Use of Laboratory Animals* with approval from Baylor College of Medicine's Institutional Animal Care and Use Committee.

Adenovirus microinjection

Ad5-CMV-Cre and Ad5-CMV-LacZ stocks were diluted to 1.0×10^{10} PFU/ml in sterile Ringer's solution and supplemented with bromophenol blue as a marker dye. This dilution was made immediately before performing intraductal injection and maintained on ice to ensure virus stability. Inguinal and thoracic mammary glands of 6-week-old mice were injected with 10 μl of Ad5-CMV-Cre virus on the right-side mammary glands or Ad5-CMV-LacZ virus on the left side as described previously (*23*). Mammary glands were harvested 2 weeks after injection, fixed in cold 4% paraformaldehyde (PFA), and processed for immunostaining.

In vivo administration of PTX

PTX was purchased from Sigma-Aldrich and reconstituted in PBS at 100 ng/μl. BrdU was purchased from Sigma-Aldrich and was reconstituted in PBS at 25 mg/ml. Six-week-old *mT-mG/SmoM2^c* mice (injected with ad-lacZ/ad-Cre) were treated with an intraperitoneal injection of PTX (300 ng/day) for two consecutive days. On the third day, the mice were pulsed with BrdU (250 mg/kg) administered intraperitoneally for 2 hours and euthanized. Mammary glands were removed, fixed in cold 4% PFA for 3 hours, and processed for immunostaining.

GANT61 administration in vivo

Gli1 and Gli2 antagonist (GANT61) was a gift from R. Toftgård. GANT61 was dissolved in a corn oil and ethanol mixture (4:1 ratio) at a concentration of 25 mg/ml. Six-week-old *mT-mG/SmoM2^c* mice (injected with ad-lacZ/ad-Cre) were treated with a subcutaneous injection of GANT61 (50 mg/kg) for three consecutive days. On the third day, the mice were pulsed with BrdU (250 mg/kg) administered intraperitoneally for 2 hours and euthanized.

Ex vivo organ culture

Mammary gland tissues from 5-week-old *mT-mG/SmoM2^c;MMTV-Cre* and wild-type control littermates were harvested and placed in Waymouth's medium (Invitrogen) to keep glands moist (*35*). Glands were then spread on a petri dish to obtain 3-mm punch biopsies containing epithelium and stroma with the aid of a fluorescence dissection stereoscope (Leica MZ16 F). Biopsies were then spread on Dacron mesh (Millipore) and incubated on the surface of Waymouth's medium supplemented with Hepes (20 mM), hydrocortisone (100 ng/ml), insulin (5 μg/ml), aldosterone (100 ng/ml), gentamicin (50 μg/ml), and antibiotic-antimycotic (1×) at 37°C for 2 days. Fresh medium with and without PTX (100 ng/ml) was added 1 day after initial culture, tissue biopsies were harvested 24 hours afterward and fixed in 4% PFA, and 3-μm tissue sections were cut for immunofluorescence staining. All samples are representative of pooled biological replicates from three experiments.

E_2 and P_4– and pregnancy-induced proliferation

Eight- to 9-week-old nulliparous, wild-type mice were injected with a single interscapular subcutaneous injection of E_2 (1 μg) and P_4 (1 mg) or sesame oil vehicle control on treatment day 1 (*36*). Mice were also treated intraperitoneally with either PTX or PBS on treatment days 1 and 2. Mice were pulsed with BrdU on day 3 and sacrificed to harvest and process tissues for histology. As a further control, we examined the effect of PTX treatment on pregnancy-induced proliferation. For timed matings, 9-week-old wild-type female mice were exposed to soiled bedding from male mice for 3 days. Thereafter, a male was added on the fourth day. Day 1 of pregnancy was determined by visualization of a vaginal mucus plug. Animals were treated with PTX or PBS on pregnancy days 4 and 5 and sacrificed on day 6 of pregnancy. Samples analyzed for the ovarian hormone and pregnancy PTX studies are representative of pooled biological replicates from five experiments in each study and were sampled randomly for the treatments received.

Mammary epithelial cell FACS and RNA isolation

Mammary epithelial cells from 9-week-old *mT-mG/SmoM2^c;MMTV-Cre* and *mT-mG/SmoM2^c;+* mice were freshly isolated using #1, #3, #4 (minus lymph node), and #5 mammary glands. The glands were then minced into 1-mm^3 fragments using a Vibratome Series 800-McIlwain Tissue Chopper and digested in collagenase A (2 mg/ml) (Roche Applied Science) in F-12 Nutrient Mixture containing antibiotic-antimycotic (Invitrogen) for 1 hour at 37°C with shaking at 200 rpm. Single cells were purified by centrifugation and trypsinization using 0.05% trypsin-EDTA (Life Technologies) as described previously (*37*). Mammary epithelial cells were suspended in Hanks' balanced salt solution supplemented with 2% fetal bovine serum and 10 mM Hepes, passed through a 40-μm filter strainer, and stained with a nonepithelial lineage panel antibody cocktail (BD Biosciences) to exclude nonepithelial cells. *mT-mG/SmoM2^c;+* (expressing tdTomato), *mT-mG/SmoM2^c;MMTV-Cre* (unrecombined; expressing tdTomato), and *mT-mG/SmoM2^c;MMTV-Cre* (recombined; expressing EGFP) mammary epithelial cells were FACS-sorted using an Aria II instrument (BD Biosciences). Total RNA was isolated from the different mammary epithelial cell populations using a Qiagen miRNeasy kit according to the manufacturer's instructions (Qiagen).

RNA sequencing

Purified double-stranded complementary DNA (cDNA) was generated from 10 ng of total RNA and amplified using both 3′ poly(A) selection and random priming throughout the transcriptome. Samples were quantified using the NanoDrop ND-1000 spectrophotometer (Thermo Scientific) and Qubit 2.0 DNA quantitation assay (Invitrogen). Each sample (3 μg) was sheared using the S2 Focused-ultrasonicator (Covaris) following the Encore NGS Library System 1 protocol (NuGEN) to obtain a final library insert size of 150 to 200 base pairs. The sheared samples were quantified using the NanoDrop ND-1000 spectrophotometer and Qubit 2.0 DNA quantitation assay. The fragment sizes were confirmed on a Bioanalyzer (Agilent Technologies) to verify proper shearing. A double-stranded DNA library was created using 200 ng of sheared, double-stranded cDNA, which prepares the fragments for hybridization onto a flowcell. This was achieved by first creating blunt-ended fragments and ligating unique adapters to the ends. The ligated products were amplified using 15 cycles of PCR. The resulting libraries were quantitated using the NanoDrop ND-1000 spectrophotometer. Library fragment size was assessed using the Bioanalyzer DNA 1000 chip (Agilent Technologies). A quantitative PCR (qPCR) quantitation was performed on the libraries to determine the concentration of adapter-ligated fragments using an iCycler iQ Real-Time PCR Detection System (Bio-Rad) and Library Quantification Kit (KAPA Biosystems).

With the concentration from the qPCR machine above, 6 pM of library was loaded onto a flowcell and amplified by bridge amplification using the cBot machine (Illumina). A paired-end 100-cycle run was used to sequence the flowcell on a HiSeq 2000 Sequencing System (Illumina).

The raw paired-end RNA-seq reads were aligned to mouse (mm9) genomes using STAR version 2.3.0e (*38*) with default settings and filtered for uniquely mapped reads. An average of about 80% of reads could be mapped; about 40 to 50% of reads were mapped to exonic regions. The normalization was performed by computing a normalization factor for each sample and each gene. A median value of the normalization factors of all the genes for each sample was selected as the normalization factor for the given sample. The normalized counts for each gene of a given sample were then transformed by asinh (*39*) (count/2), a variance-stabilizing transformation method, and plotted accordingly. Differential gene expression analysis among the three sorted cell populations [that is, *mT-mG/SmoM2^c;+*, *mT-mG/SmoM2^c;MMTV-Cre* (tdTomato), and *mT-mG/SmoM2^c;MMTV-Cre* (*EGFP*)] was performed using DESeq (*40*) by assuming that the sequencing count data follow a negative binomial distribution. *P* values were generated for each gene, and *q* values were generated from these *P* values using the Benjamini-Hochberg procedure (*41*). Each group contained four biological replicates that consisted of pooled sorted cells from five experiments. After alignment, a gene-level quality control analysis was performed using hierarchical clustering. Samples that were extreme outliers from their respective treatment groups were excluded from subsequent analysis.

The differential gene expression analysis among the three sorted cell populations described above was used to tabulate genes with increased or decreased expression in only recombined EFGP or unrecombined tdTomato mammary epithelial cells relative to wild-type tdTomato mammary epithelial cells, differentially expressed genes shared between recombined EGFP and unrecombined tdTomato mammary epithelial cells, genes with decreased expression in the recombined EFGP cells but increased expression in the unrecombined tdTomato cells, or vice versa. Furthermore, we tabulated the genes that had no difference in expression in either recombined EFGP or unrecombined tdTomato mammary epithelial cells relative to wild-type tdTomato mammary epithelial cells. The criteria for inclusion of differentially expressed genes in any of the different classifications were a pairwise fold change of twofold or greater between a pair of sorted cell populations (for example, either recombined EGFP or unrecombined tdTomato cells compared to wild-type tdTomato cells) and a *q* value as determined by the Benjamini-Hochberg method of 0.05 or less. Considering both increased and decreased expression and no change in the two comparisons between recombined EGFP and wild-type tdTomato cells or unrecombined tdTomato and wild-type tdTomato cells, there were eight total possible classes of differentially expressed genes (excluding the null class that is unchanged in both comparisons). These different classifications of differentially regulated genes were uploaded into Ingenuity Pathway Analysis in two different groups for analysis. The groups we focused on consisted of (i) genes with increased and decreased expression only in recombined EGFP cells compared to wild-type tdTomato mammary epithelial cells, (ii) genes with increased and decreased expression only in unrecombined tdTomato cells compared to wild-type tdTomato mammary epithelial cells, and (iii) genes with decreased expression in recombined EGFP cells and increased expression in unrecombined tdTomato cells.

Quantitative reverse transcription polymerase chain reaction

To evaluate the expression of mRNAs encoding Gα subunits, total RNA was isolated from FACS-sorted cells as described above. cDNA was synthesized using NuGEN's Whole Transcriptome Ovation kit per the manufacturer's instructions. TaqMan primer and probe sets and reagents were obtained from Applied Biosystems (assay ID numbers are found in table S4). qRT-PCR was performed using two independent primer and probe sets. Data were normalized to β-*actin*, and relative quantification was used to evaluate the changes in expression of mRNAs encoding $G\alpha_i$ subunits in *mT-mG/SmoM2^c;+*, *mT-mG/SmoM2^c;MMTV-Cre* (*tdTomato*), and *mT-mG/SmoM2^c;MMTV-Cre* (*EGFP*) samples. All qRT-PCR assays were run using Applied Biosystems 7500 Fast Real-time PCR system. Analysis was conducted using the ΔC_t method, and box plots with scatters were generated for visually representing data. Each group contained five biological replicates with each one having three technical replicates, which were averaged for analysis.

Immunohistochemistry

Sections (3 μm) were deparaffinized and rehydrated into PBS through a series of graded ethanols. To retrieve antigens, slides were heated in

tris-EDTA buffer at a pH of 9.0 under pressurized conditions using a decloaker (Biocare Medical). BrdU (1:200, Abcam, #ab6326) and GFP (1:250, Abcam, #ab290) were diluted in 1.5% goat serum and 8% Mouse on Mouse (M.O.M.) (Vector Laboratories) protein concentrate for background staining reduction. Slides were incubated with primary antibodies at 4°C overnight. Slides were washed in PBS supplemented with 0.04% Tween 20 and incubated with Alexa Fluor–conjugated secondary antibodies (1:500, Life Technologies, #A11007 and #A11008) for 1 hour at room temperature.

Image acquisition and processing

For in vivo and ex vivo PTX experiments, imaging was performed using a Zeiss Axioskop 2 (Zeiss Instruments) plus fluorescence microscope and AxioVision 4.8 (Zeiss MicroImaging). For in vivo experiments, the percentage of BrdU incorporation was assessed by counting ten 40× fields representative of two glands per mouse. For the ex vivo experiment, seven representative 40× fields were counted from each organ culture biopsy per group. BrdU incorporation was counted using MetaMorph imaging software (Molecular Devices), and the investigator performing the counting was blinded as to the sample or group until the quantification was completed.

Statistical analysis

Statistical analysis of the effects of PTX and GANT61 on in vivo BrdU incorporation was calculated using Wilcoxon signed rank test. Differences in BrdU incorporation as a result of PTX ex vivo treatment or ovarian hormone- and pregnancy-induced proliferation were assessed with Wilcoxon rank-sum test. DESeq (RNA-seq data) and Wilcoxon rank-sum (qRT-PCR data) tests were used to test for differences in gene expression. Differences in BrdU incorporation in the genetic experiments were tested using Wilcoxon signed rank and rank-sum tests.

SUPPLEMENTARY MATERIALS

www.sciencesignaling.org/cgi/content/full/8/394/ra92/DC1

Fig. S1. Mouse breeding schematic for genetic crosses.

Fig. S2. Effect of *SmoM2^c* expression and *Gα_i* heterozygosity on proliferation.

Fig. S3. GANT61 does not block SmoM2^c-induced proliferation.

Fig. S4. Summary of RNA-seq pathway analysis in *mT-mG/SmoM2;MMTV-Cre* (recombined EGFP) and *mT-mG/SmoM2;MMTV-Cre* (unrecombined tdTomato) MECs.

Table S1. BrdU quantification summary of the effects of PTX on steroid hormone– and pregnancy-induced proliferation in wild-type adult female mice.

Table S2. BrdU quantification summary of SmoM2^c mice with various alleles of *Gα_{i1}*, *Gα_{i2}*, or *Gα_{i3}*.

Table S3. Primers used for genotyping mice.

Table S4. TaqMan assay gene and ID numbers used for qRT-PCR.

Table S5. Genes differentially regulated in *mT-mG/SmoM2^c;MMTV-Cre* (recombined EGFP), *mT-mG/SmoM2^c;MMTV-Cre* (unrecombined tdTomato), and *mT-mG/SmoM2^c;+* (WT tdTomato) mammary epithelial cells.

REFERENCES AND NOTES

1. J. Jia, J. Jiang, Decoding the Hedgehog signal in animal development. *Cell. Mol. Life Sci.* **63**, 1249–1265 (2006).
2. A. P. McMahon, P. W. Ingham, C. J. Tabin, 1 Developmental roles and clinical significance of Hedgehog signaling. *Curr. Top. Dev. Biol.* **53**, 1–114 (2003).
3. J. Xie, M. Murone, S.-M. Luoh, A. Ryan, Q. Gu, C. Zhang, J. M. Bonifas, C.-W. Lam, M. Hynes, A. Goddard, A. Rosenthal, E. H. Epstein Jr., F. J. de Sauvage, Activating *Smoothened* mutations in sporadic basal-cell carcinoma. *Nature* **391**, 90–92 (1998).
4. J. Reifenberger, M. Wolter, R. G. Weber, M. Megahed, T. Ruzicka, P. Lichter, G. Reifenberger, Missense mutations in *SMOH* in sporadic basal cell carcinomas of the skin and primitive neuroectodermal tumors of the central nervous system. *Cancer Res.* **58**, 1798–1803 (1998).
5. J. Taipale, J. K. Chen, M. K. Cooper, B. Wang, R. K. Mann, L. Milenkovic, M. P. Scott, P. A. Beachy, Effects of oncogenic mutations in *Smoothened* and *Patched* can be reversed by cyclopamine. *Nature* **406**, 1005–1009 (2000).
6. E. Nieuwenhuis, C.-c. Hui, Hedgehog signaling and congenital malformations. *Clin. Genet.* **67**, 193–208 (2005).
7. S. Teglund, R. Toftgård, Hedgehog beyond medulloblastoma and basal cell carcinoma. *Biochim. Biophys. Acta* **1805**, 181–208 (2010).
8. M. Evangelista, H. Tian, F. J. de Sauvage, The hedgehog signaling pathway in cancer. *Clin. Cancer Res.* **12**, 5924–5928 (2006).
9. N. S. Chari, T. J. McDonnell, The sonic hedgehog signaling network in development and neoplasia. *Adv. Anat. Pathol.* **14**, 344–352 (2007).
10. M. Varjosalo, J. Taipale, Hedgehog: Functions and mechanisms. *Genes Dev.* **22**, 2454–2472 (2008).
11. M. Kasper, V. Jaks, M. Fiaschi, R. Toftgård, Hedgehog signalling in breast cancer. *Carcinogenesis* **30**, 903–911 (2009).
12. M. Fiaschi, B. Rozell, A. Bergström, R. Toftgård, Development of mammary tumors by conditional expression of GLI1. *Cancer Res.* **69**, 4810–4817 (2009).
13. R. C. Moraes, X. Zhang, N. Harrington, J. Y. Fung, M.-F. Wu, S. G. Hilsenbeck, D. C. Allred, M. T. Lewis, Constitutive activation of smoothened (SMO) in mammary glands of transgenic mice leads to increased proliferation, altered differentiation and ductal dysplasia. *Development* **134**, 1231–1242 (2007).
14. T. Tenzen, B. L. Allen, F. Cole, J.-S. Kang, R. S. Krauss, A. P. McMahon, The cell surface membrane proteins Cdo and Boc are components and targets of the Hedgehog signaling pathway and feedback network in mice. *Dev. Cell* **10**, 647–656 (2006).
15. L. Izzi, M. Lévesque, S. Morin, D. Laniel, B. C. Wilkes, F. Mille, R. S. Krauss, A. P. McMahon, B. L. Allen, F. Charron, Boc and Gas1 each form distinct Shh receptor complexes with Ptch1 and are required for Shh-mediated cell proliferation. *Dev. Cell* **20**, 788–801 (2011).
16. M. Murone, A. Rosenthal, F. J. de Sauvage, Sonic hedgehog signaling by the Patched–Smoothened receptor complex. *Curr. Biol.* **9**, 76–84 (1999).
17. S. K. Ogden, D. L. Fei, N. S. Schilling, Y. F. Ahmed, J. Hwa, D. J. Robbins, G protein Gα_i functions immediately downstream of Smoothened in Hedgehog signalling. *Nature* **456**, 967–970 (2008).
18. C. Masdeu, H. Faure, J. Coulombe, A. Schoenfelder, A. Mann, I. Brabet, J.-P. Pin, E. Traiffort, M. Ruat, Identification and characterization of Hedgehog modulator properties after functional coupling of Smoothened to G_{15}. *Biochem. Biophys. Res. Commun.* **349**, 471–479 (2006).
19. N. A. Riobo, B. Saucy, C. DiLizio, D. R. Manning, Activation of heterotrimeric G proteins by Smoothened. *Proc. Natl. Acad. Sci. U.S.A.* **103**, 12607–12612 (2006).
20. A. H. Polizio, P. Chinchilla, X. Chen, S. Kim, D. R. Manning, N. A. Riobo, Heterotrimeric G_i proteins link Hedgehog signaling to activation of Rho small GTPases to promote fibroblast migration. *J. Biol. Chem.* **286**, 19589–19596 (2011).
21. M. Barzi, D. Kostrz, A. Menendez, S. Pons, Sonic Hedgehog-induced proliferation requires specific Gα inhibitory proteins. *J. Biol. Chem.* **286**, 8067–8074 (2011).
22. D. L. DeCamp, T. M. Thompson, F. J. de Sauvage, M. R. Lerner, Smoothened activates Gα$_i$-mediated signaling in frog melanophores. *J. Biol. Chem.* **275**, 26322–26327 (2000).
23. A. P. Visbal, H. L. LaMarca, H. Villanueva, M. J. Toneff, Y. Li, J. M. Rosen, M. T. Lewis, Altered differentiation and paracrine stimulation of mammary epithelial cell proliferation by conditionally activated Smoothened. *Dev. Biol.* **352**, 116–127 (2011).
24. T. D. Russell, A. Fischer, N. E. Beeman, E. F. Freed, M. C. Neville, J. Schaack, Transduction of the mammary epithelium with adenovirus vectors in vivo. *J. Virol.* **77**, 5801–5809 (2003).
25. M. Lauth, A. Bergström, T. Shimokawa, R. Toftgård, Inhibition of GLI-mediated transcription and tumor cell growth by small-molecule antagonists. *Proc. Natl. Acad. Sci. U.S.A.* **104**, 8455–8460 (2007).
26. K. Lee, J. Jeong, M.-J. Tsai, S. Tsai, J. P. Lydon, F. J. DeMayo, Molecular mechanisms involved in progesterone receptor regulation of uterine function. *J. Steroid Biochem. Mol. Biol.* **102**, 41–50 (2006).
27. P. Chinchilla, L. Xiao, M. G. Kazanietz, N. A. Riobo, Hedgehog proteins activate pro-angiogenic responses in endothelial cells through non-canonical signaling pathways. *Cell Cycle* **9**, 570–579 (2010).
28. S. A. Vokes, H. Ji, S. McCuine, T. Tenzen, S. Giles, S. Zhong, W. J. R. Longabaugh, E. H. Davidson, W. H. Wong, A. P. McMahon, Genomic characterization of Gli-activator targets in sonic hedgehog-mediated neural patterning. *Development* **134**, 1977–1989 (2007).
29. L. Hinck, The versatile roles of "axon guidance" cues in tissue morphogenesis. *Dev. Cell* **7**, 783–793 (2004).
30. P. Strickland, G. C. Shin, A. Plump, M. Tessier-Lavigne, L. Hinck, Slit2 and netrin 1 act synergistically as adhesive cues to generate tubular bi-layers during ductal morphogenesis. *Development* **133**, 823–832 (2006).
31. G. C. Harburg, L. Hinck, Navigating breast cancer: Axon guidance molecules as breast cancer tumor suppressors and oncogenes. *J. Mammary Gland Biol. Neoplasia* **16**, 257–270 (2011).
32. A. Marusyk, D. P. Tabassum, P. M. Altrock, V. Almendro, F. Michor, K. Polyak, Non-cell-autonomous driving of tumour growth supports sub-clonal heterogeneity. *Nature* **514**, 54–58 (2014).

33. G. Li, G. W. Robinson, R. Lesche, H. Martinez-Diaz, Z. Jiang, N. Rozengurt, K.-U. Wagner, D.-C. Wu, T. F. Lane, X. Liu, L. Hennighausen, H. Wu, Conditional loss of PTEN leads to precocious development and neoplasia in the mammary gland. *Development* **129**, 4159–4170 (2002).
34. N. W. Plummer, K. Spicher, J. Malphurs, H. Akiyama, J. Abramowitz, B. Nürnberg, L. Birnbaumer, Development of the mammalian axial skeleton requires signaling through the $G\alpha_i$ subfamily of heterotrimeric G proteins. *Proc. Natl. Acad. Sci. U.S.A.* **109**, 21366–21371 (2012).
35. E. Ginsburg, B. K. Vonderhaar, in *Methods in Mammary Gland Biology and Breast Cancer Research*, M. M. Ip, B. B. Asch, Eds. (Academic/Plenum Publishers, New York, 2000), chap. 14, pp. 147–154.
36. S. L. Grimm, A. Contreras, M.-H. Barcellos-Hoff, J. M. Rosen, Cell cycle defects contribute to a block in hormone-induced mammary gland proliferation in CCAAT/enhancer-binding protein (C/EBPβ)-null mice. *J. Biol. Chem.* **280**, 36301–36309 (2005).
37. B. E. Welm, G. J. P. Dijkgraaf, A. S. Bledau, A. L. Welm, Z. Werb, Lentiviral transduction of mammary stem cells for analysis of gene function during development and cancer. *Cell Stem Cell* **2**, 90–102 (2008).
38. A. Dobin, C. A. Davis, F. Schlesinger, J. Drenkow, C. Zaleski, S. Jha, P. Batut, M. Chaisson, T. R. Gingeras, STAR: Ultrafast universal RNA-seq aligner. *Bioinformatics* **29**, 15–21 (2013).
39. G. Casella, R. L. Berger, *Statistical Inference* (Thomson Learning Australia, Pacific Grove, CA, ed. 2, 2002), p. xxviii, 660 pp.
40. S. Anders, W. Huber, Differential expression analysis for sequence count data. *Genome Biol.* **11**, R106 (2010).
41. Y. Benjamini, Y. Hochberg, Controlling the false discovery rate: A practical and powerful approach to multiple testing. *J. R. Stat. Soc. Ser. B Methodol.* **57**, 289–300 (1995).

Acknowledgments: We thank G. C. Chamness, T. G. Wensel, D. E. Lewis, and D. R. Rowley for their critiquing of the manuscript. We thank the Vector Development Laboratory at Baylor College of Medicine for providing the adenoviruses, the Lester and Sue Smith Breast Center Pathology Core for preparation of tissues for histology, and Y. M. Vasquez and F. J. DeMayo for their assistance with the decidual response experiment. **Funding:** This project was supported in part by the Genomic and RNA Profiling Core at Baylor College of Medicine with funding from the NIH National Cancer Institute (grant P30CA125123) and the expert assistance of L. D. White. The research presented in this article was supported in part by the Intramural Research Program of the NIH (Z01-ES-101643 to L.B.) and NIH grants R01-CA127857 and U54-CA149196 (to M.T.L.), 1F31CA159774 (to H.V.), and CA125123 (Dan L. Duncan Cancer Center Shared Resources). **Author contributions:** H.V. conducted all PTX experiments, assisted with RNA-seq sample preparation, performed qRT-PCR assays, performed all mouse genetic experiments, and collected samples. H.V. and M.T.L. designed the study, analyzed data, and wrote the paper. A.A.F. assisted with gene expression assays. N.F.O. and A.Q.T. assisted with the mouse genetic experiments. A.P.V. contributed to the PTX experiments and RNA-seq sample preparation. P.Y., M.-F.W., S.G.H., and C.A.S. performed statistical bioinformatic analyses. N.W.P. and L.B. provided $G\alpha_i$ mutant mice. All authors discussed the results and commented on the manuscript. **Competing interests:** M.T.L. is a manager in StemMed Holdings LP and a limited partner in StemMed Ltd. The other authors declare that they have no competing interests. **Data and materials availability:** The RNA-seq data in this article have been deposited in the National Center for Biotechnology Information's Gene Expression Omnibus (GEO) database (accession #GSE70210).

Submitted 23 January 2015
Accepted 4 August 2015
Final Publication 15 September 2015
10.1126/scisignal.aaa7355
Citation: H. Villanueva, A. P. Visbal, N. F. Obeid, A. Q. Ta, A. A. Faruki, M.-F. Wu, S. G. Hilsenbeck, C. A. Shaw, P. Yu, N. W. Plummer, L. Birnbaumer, M. T. Lewis, An essential role for $G\alpha_{i2}$ in Smoothened-stimulated epithelial cell proliferation in the mammary gland. *Sci. Signal.* **8**, ra92 (2015).

An essential role for $G\alpha_{i2}$ in Smoothened-stimulated epithelial cell proliferation in the mammary gland

Hugo Villanueva, Adriana P. Visbal, Nadine F. Obeid, Andrew Q. Ta, Adeel A. Faruki, Meng-Fen Wu, Susan G. Hilsenbeck, Chad A. Shaw, Peng Yu, Nicholas W. Plummer, Lutz Birnbaumer and Michael T. Lewis (September 15, 2015)

Science Signaling **8** (394), ra92. [doi: 10.1126/scisignal.aaa7355]